J Electroceram (2006) 17:189–195
DOI 10.1007/s10832-006-8915-3

Flux-mediated epitaxy for ferroelectric $Bi_4Ti_3O_{12}$ single crystal film growth

R. Takahashi · Y. Yonezawa · Y. Matsumoto · H. Koinuma

Received: 6 September 2005 / Revised: 3 April 2006 / Accepted: 24 April 2006
© Springer Science + Business Media, LLC 2006

Abstract We propose the "Flux-mediated epitaxy" as a novel concept for the growth of single crystalline films of incongruent, volatile, and high-temperature-melting compounds. In flux-mediated eptitaxy, by supplying materials precursors from the gas phase through the liquid flux films pre-deposited on the substrate, a quasi-thermodynamic equilibrium condition is obtained at the interface between the growing films and the flux films. This process has been demonstrated in this paper by fabricating ferroelectric $Bi_4Ti_3O_{12}$ films, which has volatile Bi oxide.

The most important step in this process is the selection of the right flux material, which is hard to predict due to the lack of an appropriate phase diagram. In order to overcome this problem, we have selected the combinatorial approach. A series of ternary flux libraries composed of two self-fluxes (Bi_2O_3 and $Bi_4Ti_3O_{12}$) and a third impurity flux were fabricated on $SrTiO_3$ (001) substrates. After that, stoichiometric $Bi_4Ti_3O_{12}$ films were grown on each of these flux libraries at a temperature presumed to melt the flux. High-throughput characterization with the concurrent X-ray diffraction method resulted in the identification of CuO containing Bi_2O_3 as the flux material for the growth of single crystalline $Bi_4Ti_3O_{12}$ films. Stoichiometric $Bi_4Ti_3O_{12}$ films fabricated by using a novel CuO containing Bi_2O_3 are qualified to be single crystalline judging from their large grain size and the electrical properties equivalent to bulk single crystal's.

Keywords Flux-mediated epitaxy · $Bi_4Ti_3O_{12}$ · Volatile materials · Flux · Combinatorial technique

R. Takahashi (✉) · Y. Yonezawa · Y. Matsumoto
Materials and Structures Laboratory, Tokyo Institute of Technology, 4259 Nagatsuda-tyo, Midori-ku, Yokohama 226-8503, Japan
e-mail: ryota.takahashi@iet.ntnu.no

R. Takahashi · H. Koinuma
National Institute of Material Science, 1-2-1 Sengen, Tsukuba, Ibaraki, 305-0047, Japan

Y. Yonezawa
Fuji Electric Advanced Technology Co., Ltd. 4-18-4 Tsukama, Matsumoto, Nagano 390-0821, Japan

Y. Matsumoto · H. Koinuma
CREST Japan Science and Technology Agency, 4-1-8 Honcho, Kawaguchi, Saitama, Japan

H. Koinuma
Department of Advanced Materials Science, School of Frontier Science, University of Tokyo, 5-1-5, Kashiwanoha, Kashiwa, Chiba 277-8568, Japan

1 Introduction

The "Flux" is an admixture to assist bulk single crystal growth. This flux is necessary for the synthesis of bulk single crystals of incongruent, volatile, and high-temperature-melting compounds [1]. In general, it is difficult to fabricate high quality single crystals without using any flux. Similarly, the high-quality-film synthesis of these incongruent and volatile compounds is also difficult. For example, even though incongruent $NdBa_2Cu_3O_{7-d}$ films can be fabricated under the optimum conditions, we still can observe many grain boundaries and defects in the cross-sectional transmission electron microscopy (TEM) and many precipitates on the film surface. As a result, the epitaxial films also look like a poly-crystalline thin film [2]. One of the possible solutions is to replace the standard thin film fabrication process of these materials for a process using the flux materials as in the bulk fabrication process of single crystals. We have developed a method and named it as "flux-mediated epitaxy" [3–5]. This

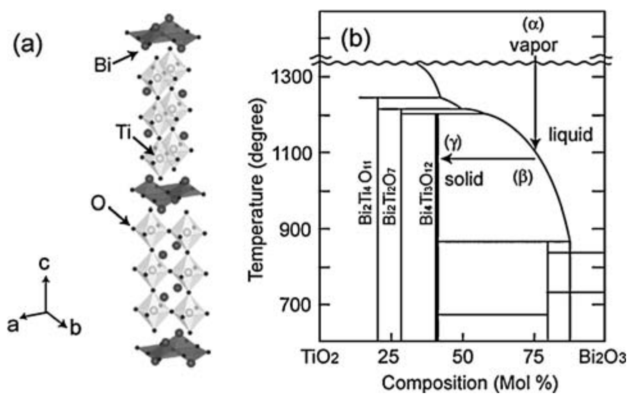

Fig. 1 (a) Schematic illustration of $Bi_4Ti_3O_{12}$ crystal structure. (b) Phase diagram of $Bi_4Ti_3O_{12}$reported in ref. 9

flux-mediated epitaxy is characterized by the dissolution of pulsed-laser ablated species into a liquid flux layer placed on the film/substrate surface and the crystallization of supersaturated species into the solid film under a quasi-equilibrium state between the growing film and the liquid flux. The crystallinity of the high T_c superconducting $NdBa_2Cu_3O_{7-\delta}$ films grown by using this method was found to be equivalent to that of the bulk single crystals of the same materials [2, 6].

We have applied this flux-mediated epitaxy for fabricating incongruent ferroelectric $Bi_4Ti_3O_{12}$ films, which include volatile Bi oxide, to demonstrate the efficiency of this method.

2 Flux-mediated epitaxy using Bi oxide self-flux

Ferroelectric $Bi_4Ti_3O_{12}$ is monoclinic with the space group B1a1 but can be considered having a highly anisotropic pseudo-orthorhombic structure with $a = 0.545$ nm, $b = 0.541$ nm and c = 3.283 nm at room temperature, as is shown in Fig. 1(a). Its spontaneous polarization vector lies in the a–c plane, with a component of 49 μC/cm ^{2} along the a-axis and 4 μC/cm^2 along the c-axis [7]. $Bi_4Ti_3O_{12}$ is an attractive material for use in nonvolatile memories and other Aurivillius phase exhibits excellent fatigue resistance during repeated polarization reversals with electric field [8]. Figure 1(b) shows the phase diagram of $Bi_4Ti_3O_{12}$, showing the incongruent melting [9]. $Bi_4Ti_3O_{12}$ bulk single crystals can be grown from Bi oxide excess region, showing that Bi oxide is a self-flux for $Bi_4Ti_3O_{12}$ growth. In order to form $Bi_4Ti_3O_{12}$ single crystal film, we firstly have used Bi oxide self-flux, supplied by the ablation of Bi excess $Bi_4Ti_3O_{12}$ (Bi: Ti = 2:1) target. The film is formed on BHF-treated $SrTiO_3$(001) substrate [10] at 800°C in 6 Torr oxygen by a KrF excimer laser ablation (248 nm, 1.8 J/cm^2, 10 Hz).

Figure 2(a) shows the atomic force microscope (AFM) of $Bi_4Ti_3O_{12}$ thin films with Bi oxide self-flux. An atomically flat surface can be observed in a large area of 10 × 10 μm. The step height is 1.6 nm, corresponding to the half unit of $Bi_4Ti_3O_{12}$ crystal structure. Figure 2(b) shows AFM image in a narrow area (1 × 1 μm) of (a). 0.4 nm step structure is observed on the $Bi_4Ti_3O_{12}$ film surface. Figure 2(c) shows AFM image of the substrate part covered with SUS mask during the film growth. We can observe atomically flat terraces steps with 0.4 nm height, corresponding to a unit of $SrTiO_3$ crystal structure. This image was taken along the same direction with Fig. 2(b). The width, height and direction of (b) are the same with those of (c). This is meaning that $Bi_4Ti_3O_{12}$ thin films grown with Bi oxide self-flux have many out-of-phase boundaries originated from substrate steps [11], as is illustrated Fig. 2(d). TEM results verified that this film had many out-of-phase boundaries [5]. Moreover, the secondary ion mass spectroscopy (SIMS) measurements showed that a high deficiency of Bi was observed, resulting in high leakage current densities, in the range of 10^{-3}–10^{-4} A/cm^2. Even if Bi oxide flux was used for $Bi_4Ti_3O_{12}$ thin film synthesis, high quality thin film could not be formed.

3 Combinatorial screening of an impurity flux

In order to solve this problem with out-of-phase boundary and volatile Bi deficiencies, we have used an impurity flux for the ideal flux-mediated epitaxy $Bi_4Ti_3O_{12}$ thin film growth. However, there has not yet been a guiding principle established to select and optimize a flux composition for a given crystal growth due to the diversity of possible flux materials. It is inevitably laborious and time-consuming to optimize the composition of the flux materials in a conventional "one-by-one" process. The combinatorial approach offers a novel and unique way to overcome these problems. Combinatorial methods are highly efficient ways to create large composition libraries of materials and test those compositions systematically in parallel for specific properties of interest, as against the time-consuming one-composition-at-a-time approach [12–14].

For screening the flux materials, ternary composition spread libraries were fabricated by use of a combinatorial pulsed laser deposition (PLD) system [13]. We designed flux libraries including a $Bi_{4+x}Ti_{3-x}O_d$ $(0 < x < 3)$ self-flux and impurity fluxes, $(MO_x)_p(Bi_4Ti_3O_{12})_q(BiO_y)_r$ library, where $M = V$, W, Cu, Mo, BiP, or Ba, $p + q + r = 1$, $0 \leq p$, q, $r \leq 1$. This ternary composition spread film was deposited directly on the substrate, and the $Bi_4Ti_3O_{12}$ film was subsequently deposited at a temperature that was expected to melt the flux.

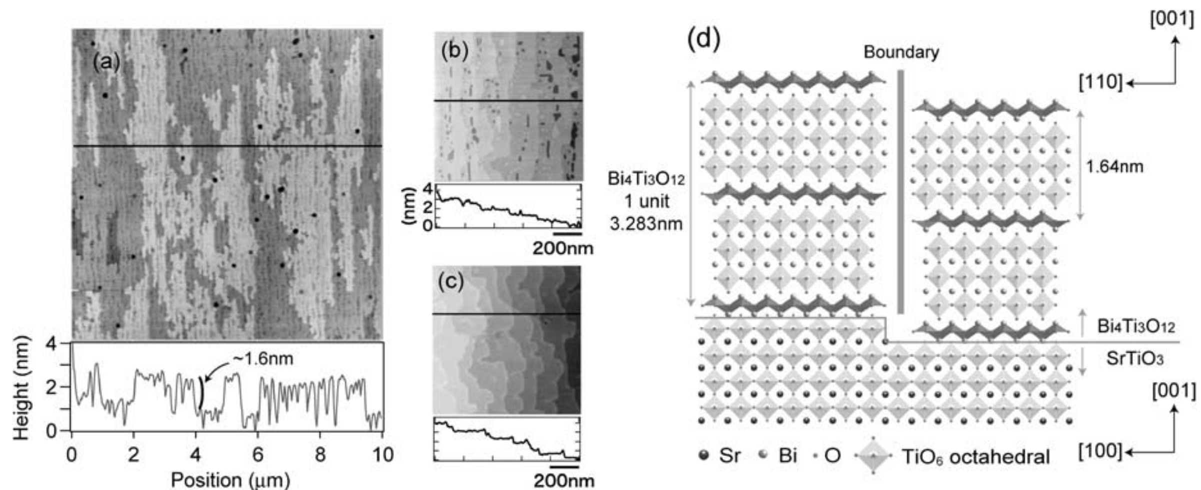

Fig. 2 (a) AFM image (wide range: $10 \times 10\,\mu$m) of $Bi_4Ti_3O_{12}$ thin films grown by PLD using Bi excess $Bi_4Ti_3O_{12}$ target. Atomically flat surface can be observed with 1.6 nm height steps, corresponding to the half unit of $Bi_4Ti_3O_{12}$ crystal. (b) AFM images in a narrow range ($1 \times 1\,\mu$m) of (a). Atomically flat film surface can be observed with "0.4 nm" height steps. (c) AFM images on the substrate covered with SUS plate during the film growth. We can observe the "0.4 nm" height steps, corresponding to a unit of $SrTiO_3$ crystal structure. Moreover, terrace width and direction are same with those in (b). (d) Schematic illustration of the formation mechanism of out-of-phase boundary in $Bi_4Ti_3O_{12}$ film

These combinatorial libraries were characterized by concurrent XRD [14]. In general, c-axis oriented $Bi_4Ti_3O_{12}$ film is grown on $SrTiO_3$(001) substrate, as is shown in Fig. 3(a). The strongest peak is $Bi_4Ti_3O_{12}$ (00$\underline{14}$) plane. We mapped this peak intensity and c-axis parameter over the entire range of $Bi_4Ti_3O_{12}$ films in addition with $Bi_4Ti_3O_{12}$ film grown without flux (Fig. 3(b)–(h)). Each of ternary libraries contains ~5000 measurement points in a triangle library with 8 mm sides. Even in the case of the $Bi_4Ti_3O_{12}$ film grown without any flux, the peak intensity and the c-axis parameter are slightly fluctuated on each measurement points. A detailed statistical analysis of the flux library allowed us to establish a clear tendency. We can see that most impurity fluxes produced poor quality $Bi_4Ti_3O_{12}$ films, except for the CuO flux. The $Bi_4Ti_3O_{12}$ films on the CuO-containing flux library showed higher X-ray intensity than any other library. Moreover, there is a tendency for the c-axis value for the $Bi_4Ti_3O_{12}$ films on the CuO-containing flux library to approach the $Bi_4Ti_3O_{12}$ bulk value (3.283 nm) reported in ref. [7]. This combinatorial screening expects that the best candidate of an impurity flux is CuO. Details in this first screening process are shown in ref. 4,5. After further optimization of several growth parameters, we finally succeeded in the preparation of a stoichiometric $Bi_4Ti_3O_{12}$ single crystal film with ultrahigh quality by using the novel CuO-containing BiO_x flux.

4 Flux-mediated epitaxy using CuO containing flux

Figure 4 shows the optimum process of flux-mediated epitaxy for $Bi_4Ti_3O_{12}$ film growth. At first, a seed $Bi_4Ti_3O_{12}$ film layer is deposited on $SrTiO_3$ (001) substrate. Subsequently, CuO flux and Bi excess $Bi_4Ti_3O_{12}$ films are deposited on the pre-deposited seed layer. Bi excess component is reacted with CuO flux, resulting in becoming a liquid layer on $Bi_4Ti_3O_{12}$ film. This CuO-containing Bi_2O_3 flux should be saturated with $Bi_4Ti_3O_{12}$ via dissolution of part of the seed layer under thermodynamic equilibrium conditions at the substrate temperature that was regulated to melt the flux. Then, laser-ablated $Bi_4Ti_3O_{12}$ fragments were supplied to the flux layer, so that the liquid flux was supersaturated, in order to re-crystallize $Bi_4Ti_3O_{12}$ film on the seed layer. During the cycle of dissolution and re-crystallization of $Bi_4Ti_3O_{12}$ grains via the liquid flux, the smaller grains were replaced by larger ones, due to the thermodynamic stability difference. Consequently, the original polycrystalline $Bi_4Ti_3O_{12}$ seed layer was also completely converted into a single crystal in (c). After deposition, the films were rapidly cooled to room temperature (d).

Figure 5 shows a laser microscope images of $Bi_4Ti_3O_{12}$ film surface with CuO containing flux (a) and no CuO flux (b), respectively. When CuO containing flux is used in the $Bi_4Ti_3O_{12}$ film deposition, we can observe the many flux precipitates on the film in (a). The total amount of all precipitates was in good quantitative agreement with that of the additional Bi_2O_3 supplied from the Bi-excess $Bi_4Ti_3O_{12}$ target during the deposition. Compositional analysis by μ-Auger electron spectroscopy (μ-AES) verified that flux precipitates were composed of CuO and Bi_2O_3. This is the direct evidence that CuO is always floated on the film surface during growth. In contrast, no precipitate was observed on the $Bi_4Ti_3O_{12}$ film grown with no CuO flux in (b). Excess

Fig. 3 (a) Shows a typical XRD pattern of c-axis oriented $Bi_4Ti_3O_{12}$ film is grown on $SrTiO_3(001)$ substrate. (b)–(h) A mapping of the c-axis lattice parameter and the $Bi_4Ti_3O_{12}(00\underline{14})$ peak intensity in no flux, V oxide, W oxide, Cu oxide, Mo oxide, BiP oxide and Ba oxide, respectively

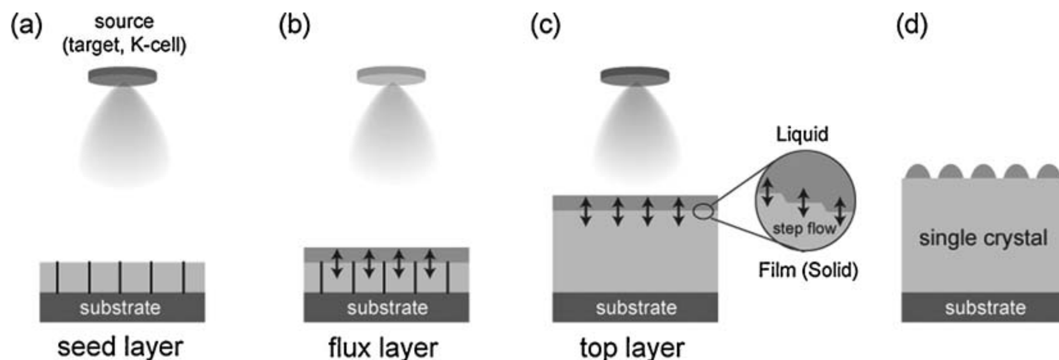

Fig. 4 Schematic illustration of the flux-mediated epitaxial process for $Bi_4Ti_3O_{12}$ single crystal film. (a) A seed $Bi_4Ti_3O_{12}$ layer is deposited from Bi-excess $Bi_4Ti_3O_{12}$ (Bi:Ti = 2:1) target on the $SrTiO_3$ (001) substrate by PLD. (b) A 20-nm-thick CuO flux layer and Bi-excess $Bi_4Ti_3O_{12}$ layer are then deposited on the seed layer. The CuO flux layer floats on the film surface even after the deposition of a Bi-excess $Bi_4Ti_3O_{12}$ layer. A Bi-excess component reacted with the CuO flux becomes the liquid flux layer. (c) Subsequent pulsed-laser ablated Bi-Ti-O species dissolve into the liquid flux layer placed on the film surface, and the supersaturated species crystallizes into the solid film under a quasi-equilibrium state between the growing film and the liquid flux. As a result, the $Bi_4Ti_3O_{12}$ film crystallinity reaches a level that is equivalent to that of the bulk single crystal. (d) After growth, the liquid flux layer is cooled and solidified as a precipitate

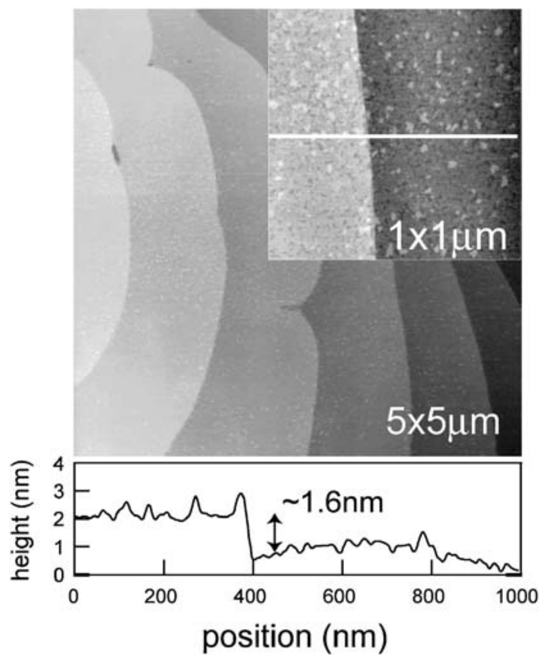

Fig. 6 AFM image of the $Bi_4Ti_3O_{12}$ film grown with CuO-containing flux

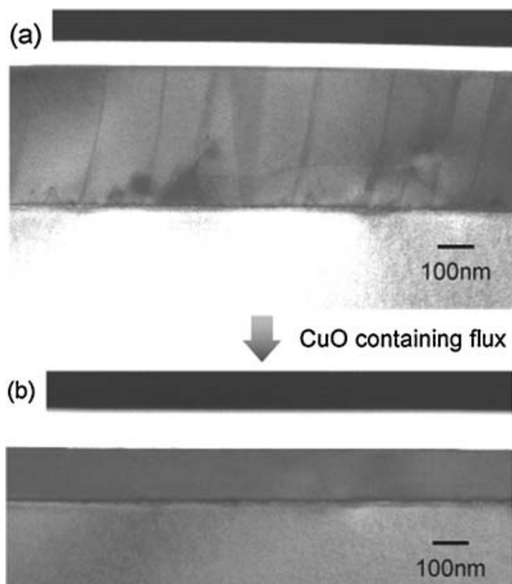

Fig. 7 TEM images of $Bi_4Ti_3O_{12}$ film grown without (a) and with CuO containing flux (b), respectively

Bi oxide component is evaporated during the film growth. This is concluded that CuO flux has an important role to suppress the volatilization of Bi oxide, so that Bi oxide flux can exist on top of the growing film.

Figure 6 shows AFM images of $Bi_4Ti_3O_{12}$ film surface with CuO containing flux. We can observe an atomically smooth terrace and steps with only 1.6 nm height, just corresponding to the half unit of $Bi_4Ti_3O_{12}$ crystal structure. The uniformity of the step height can be attributed to the uniformity of the surface-terminated layer. In fact, the terminated layer of the film was determined to be the $(Bi_2O_2)^{2+}$ layer from the cross-sectional high-resolution TEM analysis around the surface. The large terrace width should result from the equilibrium conditions prevailing at the liquid–solid interface. Furthermore, in this AFM image, $Bi_4Ti_3O_{12}$ film grown with CuO containing flux has been confirmed to have no 0.4 nm step-structures originated from out-of-phase boundaries, as is shown in Fig. 2(b). In fact, TEM analysis also verified that this film had no out-of-phase boundaries. Figure 7 shows the comparison of TEM images of $Bi_4Ti_3O_{12}$ films grown without and with CuO containing flux. Without using CuO containing flux, we can observe many ouf-of-phase boundaries in Fig. 7(a). These boundaries are originated from the step structures of substrates, as is illustrated in Fig. 2 (d) [11]. In contrast, we cannot observe any boundaries from high quality $Bi_4Ti_3O_{12}$ film grown with CuO containing flux. CuO containing flux is expected to suppress the boundary growth from the substrate steps by keeping the thermodynamic equilibrium condition at the interface, as is illustrated in Fig. 4.

The electrical properties of the $Bi_4Ti_3O_{12}$ film with CuO containing flux were also excellent. The capacitor structure was formed as is shown Fig. 8(a). Nb doped $SrTiO_3$ (Nb: 0.5 wt%) substrate was used as a bottom electrode. Pt top-electrode is deposited on the flux-free $Bi_4Ti_3O_{12}$ surface, which was etched by HCl solvent. Figure 8(b) shows the comparison of the leakage current density. Without using CuO-containing flux, the leakage current density was 10^{-3}–10^{-4} A/cm^2. This value was much higher than 10^{-7}–10^{-8} A/cm^2 of $Bi_4Ti_3O_{12}$ single crystal films grown with CuO-containing flux. This leakage current density improvement has been verified to be due to the Bi deficiencies from SIMS analysis. Without using CuO containing flux, SIMS measurements showed a high deficiency of Bi. In contrast, the composition of $Bi_4Ti_3O_{12}$ single crystal films prepared by flux-mediated epitaxy was stoichiometric: the films had Bi concentrations just corresponding to those of $Bi_4Ti_3O_{12}$ powder. Figure 8(c) shows dielectric-voltage curves measured at 1 kHz in room temperature. A conventional hysteretic butterfly loop is observed. This type of curve is typically associated with ferroelectric structures. Asymmetric pattern is originated from the difference between the bottom and top electrode. By using Sawyer-Tower test circuit [16], ferroelectric polarization hysteresis loop was also observed, showing 3 μC/cm^2 corresponding to the value of $Bi_4Ti_3O_{12}$ bulk single crystal. The improvement observed in the electrical properties of this material is therefore strong evidence for the excellent

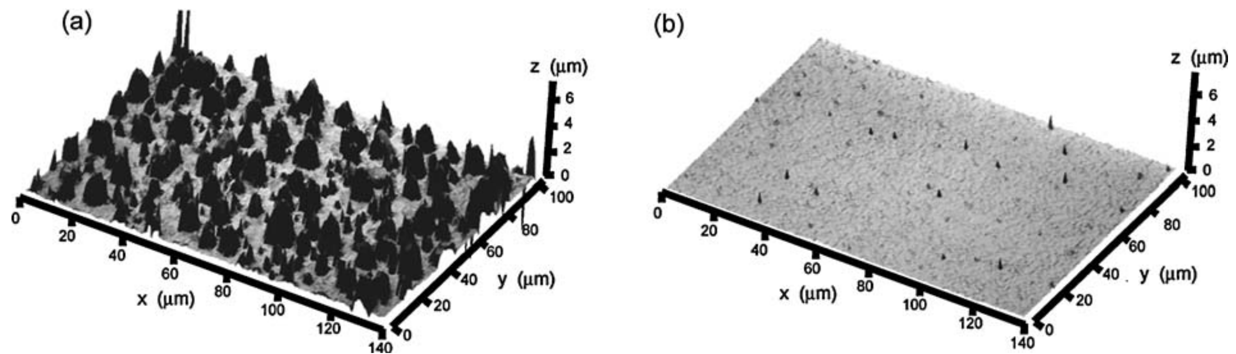

Fig. 5 (a) and (b) show laser microscope images of $Bi_4Ti_3O_{12}$ film with CuO containing flux and without CuO containing flux, respectively

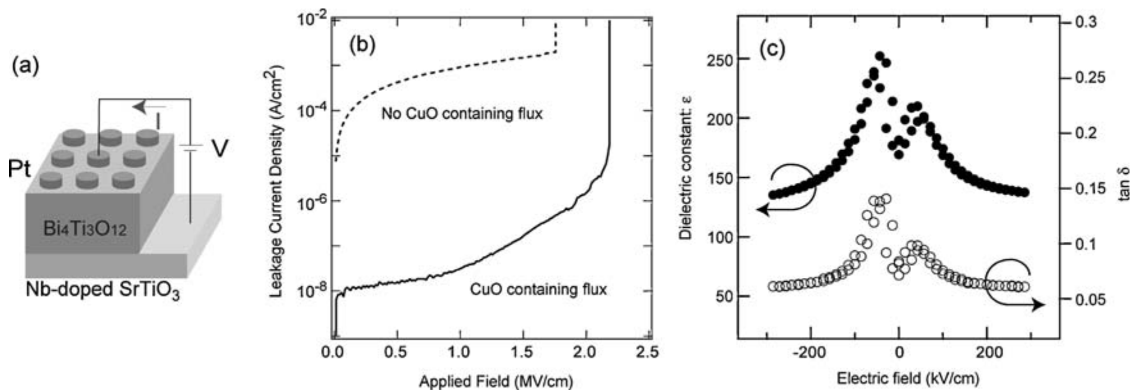

Fig. 8 Electrical properties of the $Bi_4Ti_3O_{12}$ film grown with CuO-containing flux. (a) Schematic illustration of the capacitor structure for the electric measurement. We removed the flux layer by HCl etching and subsequently deposited Pt top electrode. Conductive Nb doped $SrTiO_3$(001) substrate was used as a bottom electrode. (b) The leakage current density of $Bi_4Ti_3O_{12}$ film grown without and with CuO containing flux. (c) Dielectric-voltage curves at room-temperature. A conventional hysteretic butterfly loop is observed

crystal quality brought about by the use of flux-mediated epitaxy.

5 Conclusion

We have successfully demonstrated a great technological advantage of flux-mediated epitaxy for the single crystal quality of $Bi_4Ti_3O_{12}$ thin films by the support of combinatorial methodology. Flux-mediated epitaxy is sure to have many possibilities for the perfect single crystal epitaxy of incongruent and volatile materials, which need many optimization processes for the high quality thin film growth. The flux-mediated epitaxy is not limited to the epitaxy of oxide materials but is also widely applicable to the various materials, such as nitrides, carbides and halides, that are promising in the realization of the future non-Si-based electronics.

Acknowledgments One of the authors (R.T.) is supported by a JSPS Research Fellowship for Young Scientists. The authors would like to thank Prof. M. Kawasaki and Dr. M. Ohtani of Tohoku University for technical support in using the concurrent XRD, as well as Dr. T. Chikyow and Mrs. K. Nakajima of NIMS for technical support in using the cross-sectional TEM. The authors would also like to thank Mr. H. Watanabe, Miss Y. Ueki, Miss J. Ishii, Mr. F. Togoh, and Mr. A. Ueda of Fuji Electric Corporate R&D, Ltd., for technical support and fruitful discussions in the SIMS, XPS and μ-AES measurements.

References

1. D. Elwell and H.J. Scheel, *Crystal Growth from High-Temperature Solutions* (Academic Press, Inc., London, 1975).
2. K.S. Yun, B. D. Choi, Y. Matsumoto, J.H. Song, N. Kanda, T. Itoh, M. Kawasaki, T. Chikyow, P. Ahmet, and H. Koinuma, *Appl. Phys. Lett.*, **80**, 61 (2002).
3. Y. Matsumoto, R. Takahashi, and H. Koinuma, *J. Cryst. Growth*, **275**, 325 (2005).
4. R. Takahashi, Y. Yonezawa, M. Ohtani, M. Kawasaki, Y. Matsumoto, and, H. Koinuma, *Appl. Surf. Sci.*, **252**, 2477 (2006).
5. R. Takahashi, Y. Yonezawa, M. Ohtani, M. Kawasaki, Y. Matsumoto, and H. Koinuma, *Adv. Funct. Mater.*, **16**, 485 (2006).
6. R. Takahashi, Y. Matsumoto, H. Kohno, M. Kawasaki, and H. Koinuma, *J. Cryst. Growth*, **262**, 308 (2004).
7. Landolt-Börnstein, Ferroelectrics and Related Substances, edited by Y. Shiozaki, E. Nakamura and T. Mitsui (Springer, Berlin, Germany, 1982), Group III, Vol. 36, 9 A-15.
8. B.H. Park, B.S. Kang, S. D. Bu, T.W. Noh, J. Lee, and W. Jo, *Nature*, **401**, 682 (1999).

9. Y. Matsuda, H. Matsumoto, A. Baba, T. Goto, and T. Hirai, *Jpn. J. Appl. Phys.*, **31**, 3108 (1992).
10. M. Kawasaki, K. Takahashi, T. Maeda, R. Tsuchiya, M. Shinohara, O. Ishiyama, T. Yonezawa, M. Yoshimoto, and H. Koinuma, *Science,* **266**, 1540 (1994).
11. X.Q. Pan, J.C. Jiang, C.D. Thesis, and D.G. Schlom, *Appl. Phys. Lett.*, **83**, 2315 (2003).
12. H. Koinuma and I. Takeuchi, *Nature Materials*, **3**, 249 (2004).
13. R. Takahashi, H. Kubota, M. Murakami, Y. Yamamoto, Y. Matsumoto, and H. Koinuma, *J. Comb. Chem.*, **6**, 50 (2004).
14. M. Ohtani, T. Fukumura, M. Kawasaki, K. Omote, T. Kikuchi, J. Harada, A. Ohtomo, M. Lippmaa, T. Ohnishi, D. Komiyama, R. Takahashi, Y. Matsumoto, and H. Koinuma, *Appl. Phys. Lett.*, **79**, 3594 (2001).
15. C. B. Sawyer and C.H. Tower, *Phys. Rev.*, **35**, 269 (1930).